Ability of Iron(III)-Loaded Carboxylated Polyacrylamide-Grafted Sawdust to Remove Phosphate Ions from Aqueous Solution and Fertilizer Industry Wastewater: Adsorption Kinetics and Isotherm Studies

MAYA R. UNNITHAN, V. P. VINOD, T. S. ANIRUDHAN

Department of Chemistry, University of Kerala, Kariavattom, Trivandrum - 695 581, India

Received 18 May 2001; accepted 28 August 2001

ABSTRACT: Iron(III)-loaded carboxylated polyacrylamide-grafted sawdust was investigated as an adsorbent for the removal of phosphate from water and wastewater. The carboxylated polyacrylamide-grafted sawdust was prepared by graft copolymerization of acrylamide and *N,N′*-methylenebisacrylamide onto sawdust in the presence of an initiator, potassium peroxydisulfate. Iron(III) was strongly attached to the carboxylic acid moiety of the adsorbent. The adsorbent material exhibits a very high adsorption potential for phosphate ions. The coordinated unsaturated sites of the iron(III) complex of polymerized sawdust were considered to be the adsorption sites for phosphate ions, the predominating species being $H_2PO_4^-$ ions. Maximum removal of 97.6 and 90.3% with 2 g L^{-1} of the adsorbent was observed at pH 2.5 for an initial phosphate concentration of 100 and 250 μmol L^{-1}, respectively. The adsorption process follows second-order kinetics. Adsorption rate constants as a function of concentration and temperature and kinetic parameters, such as $\Delta G^{\pm}$, $\Delta H^{\pm}$, and $\Delta S^{\pm}$, were calculated to predict the nature of adsorption. The L-type adsorption isotherm obtained in the sorbent indicated a favorable process and fitted the Langmuir equation model well. The adsorption capacity calculated by the Langmuir adsorption isotherm gave 3.03×10^{-4} mol g^{-1} of phosphate removal at 30°C and pH 2.5. The isosteric heat of adsorption was also determined at various surface loadings of the adsorbent. The adsorption efficiency toward phosphate removal was tested using industrial wastewater. Different reagents were tested for extracting phosphate ions from the spent adsorbent. About 98.2% of phosphate can be recovered from the adsorbent using 0.1*M* NaOH. Alkali regeneration was tried for several cycles with a view to recover the adsorbed phosphate and also to restore the adsorbent to its original state. J Appl Polym Sci 84: 2541–2553, 2002

Key words: graft copolymer; iron(III)-loaded polymer; sawdust; thermogravimetric analysis; phosphate removal; adsorption; wastewater

INTRODUCTION

Although phosphorus has been conventionally regarded as a major nutrient for both plants and microorganisms, increasing attention has been focused in the last few years on the deleterious role of this element in the nutrient enrichment of streams, rivers, and lakes. Excessive growth of algae and other plants, simulated by the addition of large amounts of phosphorus to water supplies, is a problem of national concern. In addition to the excessive growth of aquatic plants and micro-

Correspondence to: T. S Anirudhan (tsani@rediffmail.com).

Journal of Applied Polymer Science, Vol. 84, 2541–2553 (2002)

organisms, the deleterious effects of eutrophication include fish kills, filter clogging, undesirable odor and taste of potable water, and a deterioration of recreational and aesthetic values.[1] The sources of phosphorus found in bodies of water may be divided into two categories—point sources, which are well-defined discharges from factories or outlets of municipal sewage systems, and diffuse sources, which include run-off from rural and urban landscapes.[2] The elimination of phosphorus from water and wastewater is important to protect public health. Among various physicochemical methods adopted for treating wastewaters, the adsorption process plays an important role in water-treatment applications. Different adsorbent materials, such as activated carbon,[3,4] activated alumina,[5] half-burnt dolomite,[6] and aluminum-impregnated coconut shell carbon,[7] have been used for the removal of phosphate from aqueous solutions.

Graft polymerization on solids followed by functionalization is now widely used for the surface modification of adsorbent materials and the products usually enhance adsorption efficiency of the adsorbent. Materials such as iron(III) oxide, silica gel, chitosan, and biomass have been used as polymer supports for the preparation of adsorbent material having different functional groups.[8,9] Adsorbents, such as polyacrylamide-grafted sawdust[10] and coconut husk[11] having carboxylate groups and polymerized coconut coir[12] with the amine functionality, have been reported to be useful for the removal of heavy metals from wastewaters. Yoshida et al.[13] reported that, of the iron(III)–loaded weakly acidic carboxylate-type cation-exchange resin, Amberlite IRC–50 was the most advantageous adsorbent for phosphate with regard to its adsorption capacity, thermal stability, iron-binding property, and recycling performance. Recently, we reported on iron(III)–loaded polyacrylamide-grafted sawdust[14] having a carboxylate group for the removal of chromium(VI) from wastewater and on evidence that the adsorbent-bound iron(III) was the site for anionic adsorption. Accordingly, the present investigation was undertaken to examine the utility of iron(III)-loaded polyacrylamide-grafted sawdust having carboxylate groups for the removal of phosphate from water and wastewater under kinetic and equilibrium conditions.

EXPERIMENTAL

Preparation of Adsorbent

The sawdust (SD) of rubber wood (*Havea braziliensis*) was obtained from a local coir industry.

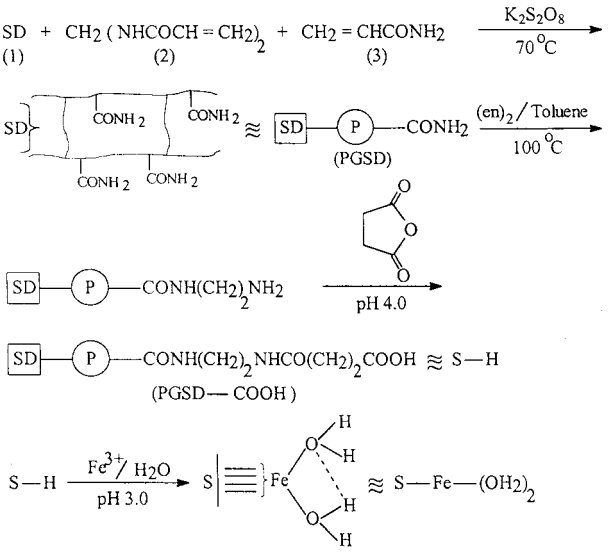

Scheme 1

The material was washed with water, dried at 80°C for 4 h, and crushed to a particle size less than 1 mm. Grafting of polyacrylamide onto SD was performed using the procedure described by Raji and Anirudhan.[10] About 20 g of SD (1) was soaked in a 300 mL solution containing 5 g of *N,N′*-methylenebisacrylamide (2) and 2 g of peroxydisulfate. To the mixture, 7.5 g of acrylamide (3) was added, and the combination was refluxed at 70°C (Scheme 1). The polyacrylamide-grafted sawdust (PGSD) was washed with water and dried at 80°C. The dried mass was refluxed with 25 mL of ethylenediamine, $(en)_2$, in toluene for 8 h, then washed with toluene and dried. To functionalize it with a carboxylate group, one part by weight of the above material was refluxed with an equal part by weight of succinic anhydride in 1,4-dioxane at pH 4.0 for 6 h.[10,11] The excess succinic anhydride was washed with 1,4-dioxane and finally with ethanol and then the product was dried. The carboxylic acid-bound polyacrylamide-grafted sawdust, PGSD–COOH, was sieved to get a 0.096-mm particle size. The physical, surface, and structural properties of PGSD–COOH were reported on in a previous article.[10] The structure of PGSD–COOH is represented in Scheme 1. The amount of the carboxylate group in PGSD–COOH was 2.03 ± 0.08 mmol g^{-1}.

To prepare an iron(III) complex of PGSD–COOH containing 1.40 mmol iron(III) per gram of adsorbent, the following procedure was applied: About 15 g of the sodium form of PGSD–COOH, which had been conditioned by successive washings

with a 1.0*M* HCl and NaOH solution, was treated with 200 mL of 0.03*M* sodium acetate–acetic acid (buffer pH 3.0) containing 10 g of iron(III) chloride hexahydrate. The iron(III)-loaded PGSD–COOH was filtered and washed with distilled water several times until all the physically adsorbed and/or absorbed iron(III) was removed and finally dried at 60°C for 6 h. Hereafter, the iron(III) complex of PGSD–COOH will be designated as S—$Fe(OH_2)_2$ (Scheme 1). The sorbent particles, having an average diameter of 0.096 mm, were used for the adsorption experiments. Even though the adsorbents [S—$Fe(OH_2)_2$] were prepared in three different batches for evaluating the reproducibility of the experimental results, all the experiments were performed using the first batch of the adsorbent.

Adsorption and Desorption Experiments

Phosphate adsorption from an aqueous solution was investigated in batch adsorption equilibrium experiments. The effects of the initial concentration and temperature on the phosphate adsorption rate were studied. Phosphate solutions of 50 mL with different concentrations were shaken with 0.1 g of the adsorbent at varying temperatures using a temperature-controlled water-bath shaker. Aliquots of the supernatant solution were withdrawn at different time intervals and the amount of phosphate in the solution was estimated by the Molybdenum Blue method.[15] The amount of adsorbed phosphate ions was calculated as $q = [(C_0 - C_A)V]/m$, where q is the amount of phosphate adsorbed onto unit amount of the adsorbent (μmol g^{-1}); C_0 and C_A, the concentrations of the phosphate ions in the initial solution and in the aqueous phase after adsorption, respectively (μmol L^{-1}); V, the volume of the aqueous phase (mL); and m, the weight of the adsorbent (g). To investigate the effect of pH on adsorption, a pH study was carried out by agitating 50 mL of 100 and 250 μmol L^{-1} phosphate solutions with 100 mg of the adsorbent at different pH values (2–10) for 4 h. The pH of the solution was adjusted using 0.1*M* NaOH and HCl. For studying adsorption isotherms at pH 2.5, a phosphate concentration range between 100 and 2500 μmol L^{-1} was used and the temperature of the test solution was varied in the range of 30–60°C at intervals of 10°C. The adsorption of phosphate ions from a fertilizer industry wastewater sample was also performed in a batchwise manner. Fifty milliliters of a solution containing 250 μmol L^{-1} was treated with different amounts of the adsorbent at 30°C. After adsorption, the concentration of phosphate in the supernatant was obtained using the method described earlier.

After the adsorption experiments, the phosphate-laden adsorbent, separated by filtration, was gently washed with distilled water to remove any unadsorbed phosphate ions. The spent samples (0.1 g) were agitated with 50 mL of desorbing reagents. The desorbed phosphate ions were estimated by analyzing the desorbing medium. The percentage of desorption was determined from the amount of phosphate initially loaded onto the adsorbent and the final phosphate concentration in the desorbing medium. To determine the reusability of the adsorbent, consecutive adsorption–desorption cycles were repeated three times using the same adsorbent.

All the experiments were done in duplicate or triplicate and were also reproduced on different days. The maximum variation in the batch-adsorption data between duplicate/triplicate experiments done on the same day was 4.2% and that between experiments done in two different days was 5.0%. To evaluate the kinetic and mechanistic parameters associated with the adsorption process, the experimental data were treated after discarding the data that lay outside the 95% confidence interval, which was established by a method of least squares for the linear function. The uncertainty of the parameters of the adjusted straight line corresponds to the standard deviations.

RESULTS AND DISCUSSION

Adsorbent Characterization

The iron(III) content in the adsorbent was determined spectrophotometrically[15] on acid eluate and was found to be 1.40 mmol g^{-1}. To determine whether there is any dissolution of iron from the adsorbent during the adsorption and desorption processes, the supernatant solution was analyzed for both iron(II) and iron(III). It was observed that iron(III) is strongly bound to the resin, so that it is not easily released from the adsorbent even in the presence of the alkali and alkaline earth metal cations above pH 3.0.

The Viladker et al.[16] method of Methylene Blue (MB) adsorption was employed to measure the specific surface area of the adsorbent. The adsorption of MB on S—$Fe(OH_2)_2$ as a function of the

initial concentration at 30°C was studied by the addition of 50 mL (1.34×10^{-5} to 2.67×10^{-4} *M*) solution to 0.1 g of S—$Fe(OH_2)_2$. After an equilibration of 24 h, the supernatant was decanted off and the concentration of MB was determined spectrophotometrically at 660 nm. The adsorption isotherm data thus obtained are depicted in Figure 1. The specific surface area of the adsorbent was derived using the following equation:

$$S_s = (M_f N/10^5)A_m 10^{-20} \quad (\mathrm{m^2\ g^{-1}}) \qquad (1)$$

where M_f is the amount of MB (μmol) adsorbed per 100 g of the adsorbent when the surface is completely covered with a monolayer of MB; N, the Avogadro number; and A_m, the cross-sectional area per molecule on the surface (130 A^2). The value of M_f was obtained from the MB adsorption isotherm (Fig. 1) after extrapolating the "knee point" to the q_e axis and taken as the point of monolayer coverage. Substitution of the extrapolated point, M_f, in the above equation gave the value of the specific surface area of the adsorbent.

The zero-point charge, pH_{zpc}, is defined as the pH of the suspension at which the surface charge density $\sigma_0 = 0$. σ_0, as a function of pH and ionic strength on S—$Fe(OH_2)_2$, was determined using a potentiometric method.[17] σ_0 was computed from the above data using the following equation:

$$\sigma_0 = \frac{F(C_A - C_B + [\mathrm{OH^-}] - [\mathrm{H^+}])}{A} \qquad (2)$$

where σ_0 is in Coulomb per square centimeter units; A, the total surface area in suspension (cm^2 L^{-1}); and C_A and C_B, the concentrations of acid and alkali after each addition during titration (eq L^{-1}). F is the Faraday constant (C eq^{-1}) and $[H^+]$ and $[OH^-]$ are the equivalents of H^+ and OH^- ions bound to the suspension surface (eq cm^{-2}). The experimental titration curves at different ionic strengths (0.001, 0.01, and 0.1*M* $NaNO_3$) as a function of the pH is shown in Figure 2. The results clearly demonstrate that pH influences the surface charge. This implies that OH^- and H^+ ions are the potential determining species and that the surface charge is developed in accordance with Figure 4. The results also suggest that Na^+ and NO_3^- ions were not significantly adsorbed by the adsorbent. The point of intersection of the σ_0 versus the pH curve (Fig. 2) showed that the pH_{zpc} of the adsorbent occurred at 9.2.

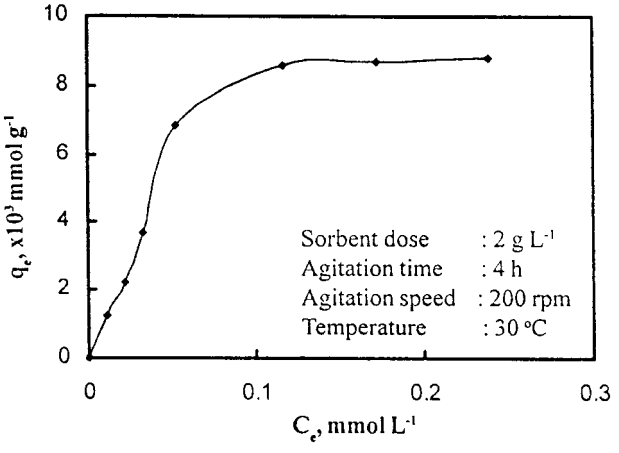

Figure 1 Adsorption isotherm of MB on S—$Fe(OH_2)_2$.

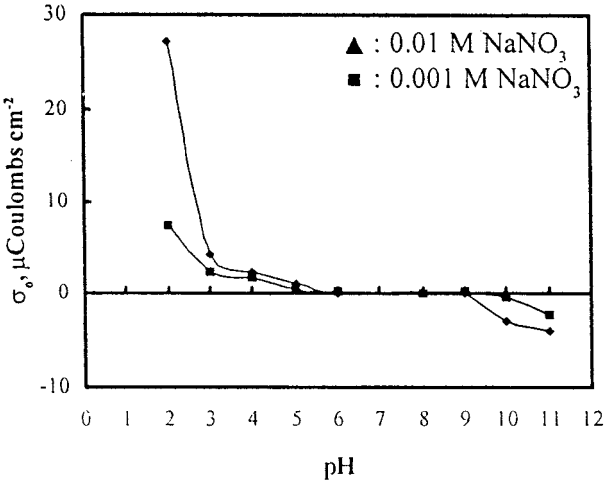

Figure 2 Surface charge density as a function of pH in aqueous solution of $NaNO_3$.

Simultaneous thermogravimetric (TG) and differential thermal analysis (DTA) were carried out on a Mettler Toledo Star TG–DTA instrument at a heating rate of 20°C/min. The TG curve (Fig. 3) showed an initial small weight loss (2% of the sample), starting at 80°C and ending at 110°C, due to the loss of physically adsorbed water (moisture content). Then, a break (temperature range 120–180°C) in the thermogram indicates the loss of water molecules, which are possibly associated (coordinated) with the carboxylate group on the adsorbent surface. The DTA curve shows a sharp endothermic peak in the range 90–160°C, coinciding with the loss of both physically adsorbed and coordinated water in the adsorbent system. To determine the thermal stability trend for polymeric material, thermogravimetric parameters, such as temperature for 10% weight loss (T_{10}) and

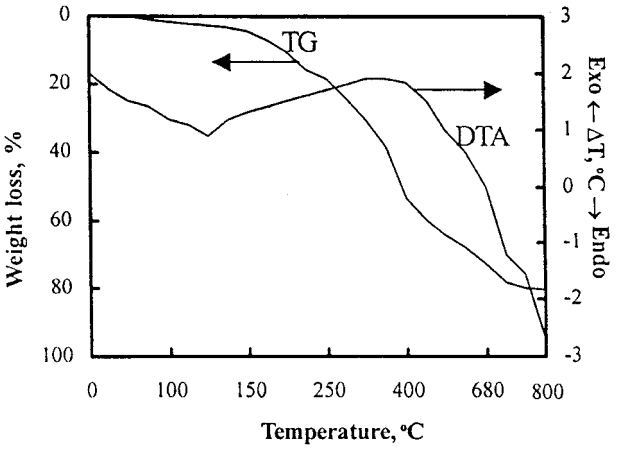

Figure 3 TG and DTA curves of S—$Fe(OH_2)_2$.

the temperature of maximum rate of degradation (T_{max}), were calculated by methods reported earlier.[18] T_{10} and T_{max} are the two main criteria used to indicate the heat stability of polymers. The higher the value of T_{10} and T_{max}, the higher is the thermal stability of the system.[19] The values of T_{10} and T_{max}, found to be 195 and 410°C, respectively, indicate the high thermal stability of the adsorbent.

The characteristics of the adsorbent prepared in first batch are as follows: surface area, 68.71 ± 3.40 $m^2\ g^{-1}$; pH_{zpc}, 9.2 ± 0.5; apparent density, 1.68 ± 0.08 g mL^{-1}; porosity, 0.44 ± 0.04 mL g^{-1}; water content, 6.47 ± 0.32 mmol g^{-1}; iron content, 1.40 ± 0.05 mmol g^{-1}; and polymer content, 21.8 ± 1.2%. The adsorbent was used to study the effect of the pH, initial concentration of the adsorbate, temperature, adsorbent dose, diverse ions, etc., on the removal efficiency of phosphate. The experimental results and the relevant observations are discussed in the following sections.

Effect of Adsorbent Dose on Phosphate Adsorption

The adsorbent dosage is an important parameter because this determines the capacity of an adsorbent for a given initial concentration of the adsorbent. The effect of the adsorbent dosage (adsorbent prepared in different batches) was studied on phosphate removal, keeping all other experimental conditions constant (Table I). The data show that as the adsorbent dosage increases the percentage adsorption also increases, but the amount adsorbed per unit mass of the adsorbent decreases considerably. The decrease in unit adsorption with increase in the dose of the adsorbent may be attributed to the fact that some of the adsorption sites remain unsaturated during the adsorption process, whereas the number of available adsorption sites increases by increasing the adsorbent dose and that results in the increase of removal efficiency.[20] It can be observed from the table that S—$Fe(OH_2)_2$ prepared in different batches gives reproducible data with identical experimental conditions.

Effect of pH on Phosphate Adsorption

To optimize the pH for maximum removal efficiency, experiments were conducted with 50 mL of 100 and 250 μmol L^{-1} of a phosphate solution containing 0.1 g of the adsorbent in the pH range 2–10 and the results are depicted in Figure 4. The removal of phosphate by the adsorbent is very high at a low pH range, 2.0–3.5. Above this pH range, adsorption gradually decreases with increasing basicity of the medium. At pH 10.0, removal of about 17.1 and 14.0% was observed for initial concentrations of 100 and 250 μmol L^{-1}, respectively; the maxima removal of 97.6 and 90.3% were observed at pH 2.5 for the same initial concentrations. Similar pH effects were observed

Table I Effect of Adsorbent (Prepared in Different Batches) Dosage on Phosphate Adsorption

	Adsorption		
Adsorbent Dose (g L^{-1})	1st Batch [μmol g^{-1} (%)]	2nd Batch [μmol g^{-1} (%)]	3rd Batch [μmol g^{-1} (%)]
1	228.30 (76.1)	230.40 (76.8)	227.70 (75.9)
2	130.95 (87.3)	132.15 (88.1)	131.40 (87.6)
4	71.40 (95.2)	72.08 (96.1)	71.25 (95.0)
6	49.05 (99.1)	49.20 (99.4)	48.60 (98.2)
8	37.50 (100.0)	37.50 (100.0)	37.50 (100.0)

Phosphate concentration, 300 μmol L^{-1}; pH, 2.5; agitation time, 4 h; temperature, 30°C.

by Yoshida et al.[13] in the adsorption of phosphate by iron(III)-loaded Amberlite IRC. They reported that the adsorbent was effective for the quantitative removal of phosphate over the pH range 2.5–4.0 with a maximum at pH 2.5. They also demonstrated the practicality of the adsorbent material for treating wastewater streams. Vujkovic et al.[21] also reported on the capability of surfactant-modified clinoptilolite for the removal of phosphate from aqueous solutions in acidic medium in the pH range 3.5–4.5. Moreover, wastewater streams from fertilizer industries are characterized[22] as having low pH (also containing excess phosphate, fluoride, ammonia, nitrate, etc.). Hence, S—$Fe(OH_2)_2$ can be used to treat real industrial wastewater without any investment toward the chemical cost for pH adjustments.

Earlier workers[13] demonstrated that iron(III) ions, which are coordinately hexavalent, were bound to the chelating resin under so-called coordination unsaturated conditions, leaving two coordinating sites as adsorption sites for the coordinating anions. The effect of pH on phosphate removal by S—$Fe(OH_2)_2$ seems to change with the species of phosphate in the solution and the adsorption reaction. The pH_{zpc} of S—$Fe(OH_2)_2$ was found to be 9.2, and below this pH, surface charge of the adsorbent is positive. At pH 2.5, the predominant phosphate species is $H_2PO_4^-$ and, therefore, the uptake of phosphate at optimum pH is the ligand-exchange mechanism. The adsorption of phosphate can be considered to be by the ligand-exchange reaction between coordinated water and $H_2PO_4^-$ ions:

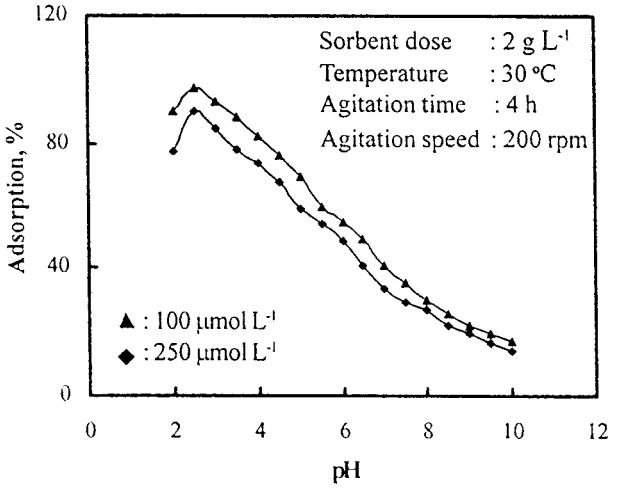

Figure 4 Effect of pH on the adsorption of phosphate on S—$Fe(OH_2)_2$.

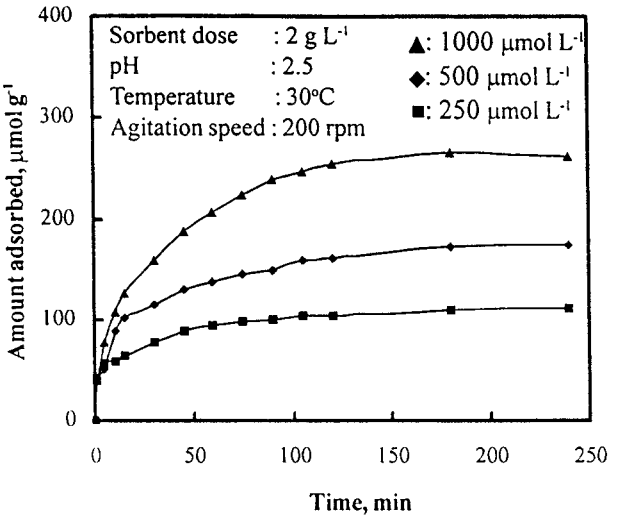

Figure 5 Effect of contact time and initial concentration on the adsorption of phosphate on S—$Fe(OH_2)_2$.

$$S—Fe(OH_2)_2 + H_2PO_4^- \rightleftharpoons S—Fe(H_2PO_4)^- + 2H_2O \quad (3)$$

A slight decrease in the percentage removal below pH 2.5 may be ascribed to the increasing concentration of phosphoric acid (H_3PO_4; $pK_1 = 2.1$), which is not adsorbed. At a higher pH range, the decrease in removal efficiency may be due to the protolysis of hydrated water on the adsorbent-bound iron. The higher concentration of OH^- ions present in the reaction mixture at higher pH competes with phosphate species (PO_4^{3-}) for the adsorption sites. As the adsorbent surface (pH $>$ pH_{zpc}) is negatively charged as well, the increasing electrostatic repulsion between negatively charged PO_4^{3-} ions and negatively charged sorbent particles would also lead to a decrease in adsorption of phosphate ions.

Effect of Initial Concentration and Agitation Time

To determine how much time is required for the adsorption process to reach equilibrium at room temperature, adsorption over a range of 1 min to 6 h using S—$Fe(OH_2)_2$ was measured. The phosphate adsorption capacities of S—$Fe(OH_2)_2$ are given as a function of time for different initial concentrations of the adsorbate in Figure 5. From these plots, it is shown that an initial fast step completed within 30 min was followed by a slow second stage. The high uptake at the initial stage may be attributed to a fast reaction taking place at the surface of the solid. The initial rapid ad-

sorption was probably a high-energy adsorption associated with low surface saturation. The slow reaction was assumed to be a result of an increased negative surface charge, increased interaction energy, and decreased adsorption energy.[23] It is also observed from the above plots that the amount of adsorption significantly increased with the initial concentration of phosphate; however, the percentage adsorption decreased. It is also observed that the agitation time needed to reach equilibrium is 4 h, after which there is no change in adsorption. The saturation period of the adsorption is extremely independent of the initial concentration. With increase in the initial concentration of phosphate from 250 to 1000 μmol L^{-1}, the uptake of phosphate decreased from 90.3% (112.88 μmol g^{-1}) to 52.2% (261.00 μmol g^{-1}). This obviously shows that the percentage adsorption of phosphate is dependent on the initial concentration. This is because, at a high initial concentration, the ratio of the initial number of moles of phosphate to the available adsorption sites is high; hence, the fractional adsorption becomes dependent on initial concentration.

Kinetics of Adsorption

The kinetics of adsorption describes the solute uptake, which, in turn, governs the residence time of the adsorption reaction. It is one of the important characteristics in defining the efficiency of adsorption. The kinetics of phosphate removal by adsorption was carried out to understand the behavior of the adsorbent developed in the present study. The adsorption of phosphate from the liquid phase to the solid phase can be considered as a second-order reaction, that is, the adsorption rate constant, k_{ad}, was obtained by assuming[24] that

- The desorption rate is small compared to the adsorption rate;
- The surface site concentration is expressed in the unit of the phosphate concentration;
- The rate of adsorption may be approximated as equal to the rate of decrease in the concentration of the sorbate solution, that is, $k_{ad} = -dc/dt$; and
- There is a monolayer of adsorbate species on the adsorbent, that is, adsorption follows the Langmuir equation.

The following integrated rate expression[24] is used to calculate the second-order rate constant (k_{ad}) values:

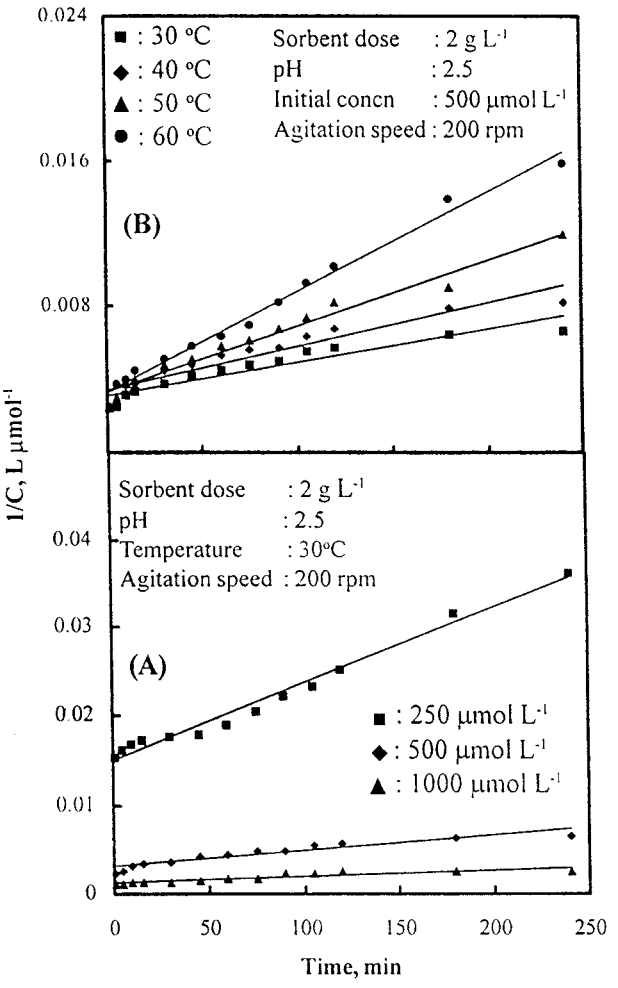

Figure 6 Second-order kinetic plots for the adsorption of phosphate on S—$Fe(OH_2)_2$ at different (A) concentrations and (B) temperatures.

$$\frac{1}{C} - \frac{1}{C_0} = k_{ad}t \qquad (4)$$

where C_0 is the initial bulk concentration of the adsorbate solution, and C, the concentration in the aqueous phase at time t. The linear plots of $1/C$ versus t (Fig. 6), for different concentrations and temperatures, indicate the validity of the above equation for the present system. The regression coefficients for the linear plots were greater than 0.98. At 30°C and pH 2.5, the k_{ad} values at the initial concentrations of 250, 500, and 1000 μmol L^{-1} were 86.0, 18.3, and 7.3 L mol^{-1} min^{-1}, respectively. The k_{ad} values at different temperatures were also calculated using regression analysis and found to be 18.3, 24.0, 36.2, and 55.7 L mol^{-1} min^{-1} at 30, 40, 50, and

60°C, respectively. The findings clearly indicate that the higher temperatures favor phosphate removal by adsorption on S—$Fe(OH_2)_2$.

The energetics of the adsorption process were also examined by temperature studies. Arrhenius[25] showed that the rate constants, k_{ad}, could be related to the temperature by the following relationship:

$$\ln k_{ad} = -\frac{E_a}{RT} + \text{constant} \quad (5)$$

The value of the activation energy E_a, as calculated from the slope of the ln k_{ad} versus $1/T$ plot, was 31.131 kJ mol^{-1}. The relatively low E_a value suggests that phosphate adsorption is by an activated or a diffusion-controlled process. Owing to the porous nature of the adsorbent, intraparticle diffusion (pore diffusion) is supposed to be the rate-limiting step. Knocke and Hemphill[26] stated, that since diffusion is an endothermic process, the rate of adsorption will increase with an increased solution temperature when pore diffusion is the rate-limiting step. Hence, results of the study on the temperature effect indicate that phosphate adsorption on S—$Fe(OH_2)_2$ is controlled by pore diffusion.

Other kinetic parameters were calculated using the following equations. According to Griffin and Jurinak,[27] the rate constant of adsorption k_{ad} can be written as

$$k_{ad} = \frac{KT}{h} e^{\Delta S^{\neq}/R} e^{-\Delta H^{\neq}/RT} \quad (6)$$

where K is the Boltzmann constant; h, the Planck constant; T, the absolute temperature; $\Delta S^{\pm}$, the entropy of activation; $\Delta H^{\pm}$, the enthalpy of activation; and R, the gas constant. The enthalpy of activation $\Delta H^{\pm}$ can be calculated using the relationship

$$\Delta H^{\neq} = E_a - RT \quad (7)$$

The entropy of activation, $\Delta S^{\pm}$, was calculated using eq. (6). The free energy of activation, $\Delta G^{\pm}$, was calculated from

$$\Delta G^{\neq} = \Delta H^{\neq} - T\Delta S^{\neq} \quad (8)$$

The values of $\Delta H^{\pm}$ and $\Delta S^{\pm}$ for the adsorption of phosphate were 28.615 kJ mol^{-1} and -126.434 J mol^{-1} K^{-1}, respectively. The positive value of $\Delta H^{\pm}$ suggests the endothermic nature of the process. The negative value of $\Delta S^{\pm}$ indicates a greater order of reaction during the adsorption of the phosphate ions. During the adsorption process, the coordinated water molecules, which are displaced by phosphate species, gain less translational entropy than is lost by the phosphate species, resulting in decreased randomness in the phosphate–S—$Fe(OH_2)_2$ interaction. The values of $\Delta G^{\pm}$ were 66.925, 68.189, 69.453, and 70.718 kJ mol^{-1} at 30, 40, 50, and 60°C, respectively. The adsorption is endothermic; hence, the amount adsorbed at equilibrium must increase with an increase in temperature, because the free energy of activation increases with increase in the temperature of a solution. This explains why the values of $\Delta G^{\pm}$ increase with an increase in temperature.

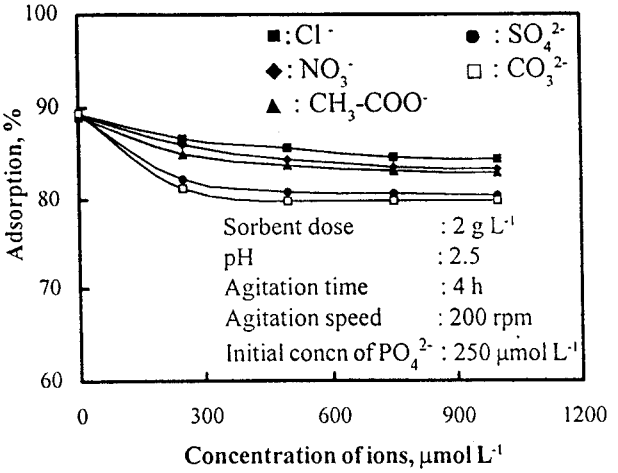

Figure 7 Effect of diverse ions on the adsorption of phosphate on S—$Fe(OH_2)_2$.

Effect of Diverse Ions

To examine the effect of acetate, sulfate, nitrate, carbonate, and chloride on phosphate uptake by S—$Fe(OH_2)_2$, experiments were conducted with different concentrations (250, 500, 750, and 1000 μmol L^{-1}) using sodium salt. A 50-mL solution containing 250 μmol L^{-1} of phosphate at pH 2.5 was agitated with 0.1 g of adsorbent for 4 h. The results are presented in Figure 7. The percentage adsorption of phosphate from the solution was 90.3 % in the absence of any anions studied. The results show that the diverse ions studied have either no interference or very little interference with the adsorption of phosphate by S—$Fe(OH_2)_2$. The interferences were at a maximum, in the case of carbonate (phosphate removal 80.2%) at a concentration of 1000 μmol L^{-1}.

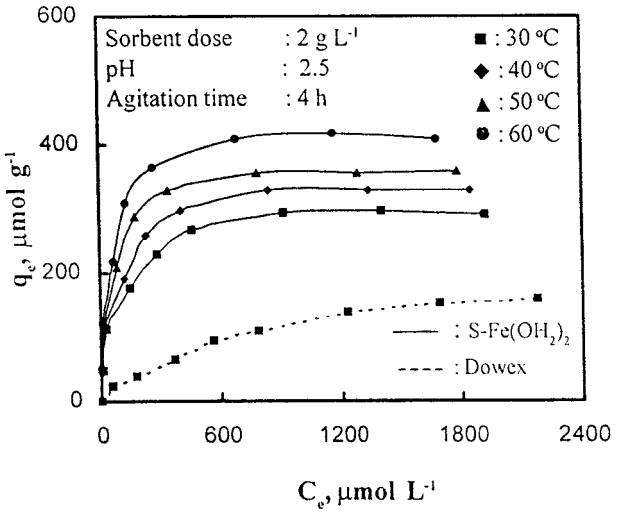

Figure 8 Adsorption isotherms of phosphate on S—$Fe(OH_2)_2$ and Dowex.

Effect of Temperature on the Adsorption Isotherm

The effect of temperature on the adsorption of phosphate onto S—$Fe(OH_2)_2$ at 30, 40, 50, and 60°C was studied for the concentration range between 100 and 2500 μmol L^{-1}. The experimental results for the adsorption isotherms are presented in Figure 8. The isotherms are concave to the y-axis up to 292.8 μmol g^{-1} at 30°C, 328.3 μmol g^{-1} at 40°C, 356.7 μmol g^{-1} at 50°C, and 410.0 μmol g^{-1} at 60°C. The L-type nature of the curve obtained in the present investigation is favorable for adsorption and indicates a strong tendency in the process for monolayer formation.[28] Adsorption isotherms tend to define a plateau; therefore, it seems reasonable to suppose that, under the experimental conditions used, the formation of a complete monolayer of phosphate ions covering the adsorbent is possible and the curves tend to a constant value of q_e. The isotherm data for the removal of phosphate by adsorption at all temperatures were fitted in the rearranged Langmuir isotherm:

$$\frac{C_e}{q_e} = \frac{C_e}{Q^0} + \frac{1}{Q^0 b} \tag{9}$$

where C_e and q_e are the equilibrium phosphate concentrations in the liquid (μmol L^{-1}) and solid (μmol g^{-1}) phases, respectively, and Q^0 and b are Langmuir constants related to the maximum adsorption capacity (mol g^{-1}) and energy of adsorption (L mol^{-1}), respectively. The linear plots of C_e/q_e versus C_e (Fig. 9) at different temperatures indicate the applicability of the Langmuir adsorption isotherm. The values of Q^0 and b for different temperatures were calculated using the least-squares method through a regression analysis and are presented in Table II along with 95% confidence limiting values and their coefficients of correlation[29] (r^2). The values of Q^0 and b increased with an increase of temperature, showing that the adsorption capacity and the intensity of adsorption are enhanced at higher temperature.

Comparison with Other Adsorbents

To justify the viability of a treatment process, the adsorption capacity of the adsorbent material must be compared with other adsorbents examined for the treatment of phosphate. The Q^0 value for the adsorption of phosphate at 30°C was reported by Sreenivasalu et al.[4] at 1.86×10^{-5} mol g^{-1} for activated carbon. For phosphate adsorption on peat[30] and red mud gypsums,[31] the values of Q^0 were reported to be 3.12×10^{-6} and 5.34×10^{-5} mol g^{-1}, respectively. Comparison of the Q^0 value of phosphate adsorption onto S—$Fe(OH_2)_2$ with the literature data indicated that the adsorption capacity of S—$Fe(OH_2)_2$ is 16.3, 97.1, and 5.8 times greater than that of the activated carbon, peat, and red mud gypsum, respectively. However, the value of Q^0 was about 2.3 times greater in iron(III)-loaded [Fe(III) content = 1.34 mmol g^{-1}] Amberlite IRC[13] ($Q^0 = 6.90 \times 10^{-4}$ mol g^{-1}) than in S–$Fe(OH_2)_2$. The difference in behavior may be due to the difference in the ligand-exchange behavior and the nature of

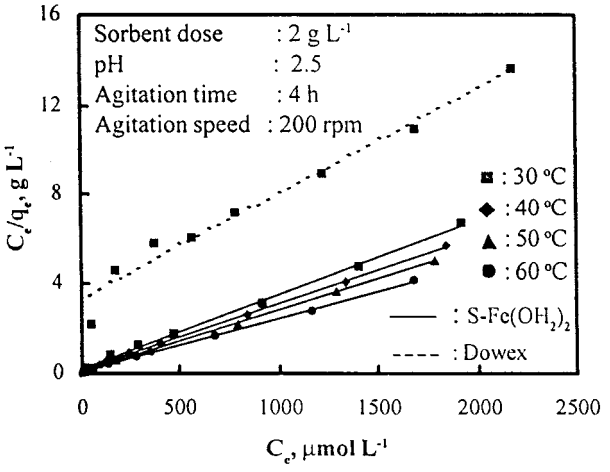

Figure 9 Langmuir isotherm plots for the adsorption of phosphate on S—$Fe(OH_2)_2$ and Dowex.

Table II Langmuir Constants for the Adsorption of Phosphate onto S—$Fe(OH_2)_2$ at Different Temperatures

Temperature (°C)	Q^0 (mol g^{-1})	95% Confidence Limit	b (L mol^{-1})	95% Confidence Limit	r^2
30	3.03×10^{-4}	2.69×10^{-4}–3.18×10^{-4}	1.68×10^4	1.50×10^4–1.79×10^4	0.96
40	3.40×10^{-4}	3.14×10^{-4}–3.70×10^{-4}	1.84×10^4	1.63×10^4–2.01×10^4	0.94
50	3.68×10^{-4}	3.40×10^{-4}–3.82×10^{-4}	2.59×10^4	2.41×10^4–2.89×10^4	0.95
60	4.21×10^{-4}	3.88×10^{-4}–4.34×10^{-4}	3.18×10^4	3.02×10^4–3.40×10^4	0.98

the resin matrices. An adsorption isotherm study was also conducted to determine the adsorption capacity of a commercial synthetic polymer-based anion-exchange resin. For this, a commercial chloride-form anion exchanger, Dowex, was supplied by Aldrich (Milwaukee, WI). Dowex has a quaternary amine functionality and ion-exchange capacity of 4.2 meq g^{-1}. No pretreatment was done on Dowex, which was used as obtained. Experimental isotherm data are shown in Figure 8. Equilibrium isotherm data at a controlled pH of 2.5 and a temperature of 30°C were also correlated using the Langmuir adsorption model. The maximum adsorption capacity Q^0 and binding constant b of Dowex at 30°C were calculated from the Langmuir plot (Fig. 9) and were 2.09×10^{-4} mol g^{-1} and 1.50×10^3 L mol^{-1}, respectively, which are considerably lower than are those of the newly developed adsorbent material.

Isosteric Heat of Adsorption

Information concerning the magnitude of the heat of adsorption, and its variation with surface coverage/loading, can provide useful information concerning the nature of the surface and the adsorbed molecules. The heat of adsorption determined at a constant amount of sorbate adsorbed is known as the isosteric heat of adsorption (ΔH_x) and was calculated using the Clausius–Clapeyron equation[32]:

$$\frac{\partial(\ln C_e)}{\partial t} = -\frac{\Delta H_x}{RT^2} \tag{10}$$

The equilibrium concentration C_e, at a constant amount of adsorbed phosphate, was obtained from the adsorption isotherm data (Fig. 8) at different temperatures. ΔH_x was calculated from the plot of ln C_e versus $1/T$ for different surface loadings (Fig. 10). ΔH_x values are shown in Figure 11 as a function of the amount of phosphate adsorbed. As shown in Figure 11, the isosteric heat of adsorption varied with the surface loading, indicating that the S—$Fe(OH_2)_2$ used has an energetically heterogeneous surface. The variation of ΔH_x with surface loading is usually attributed to

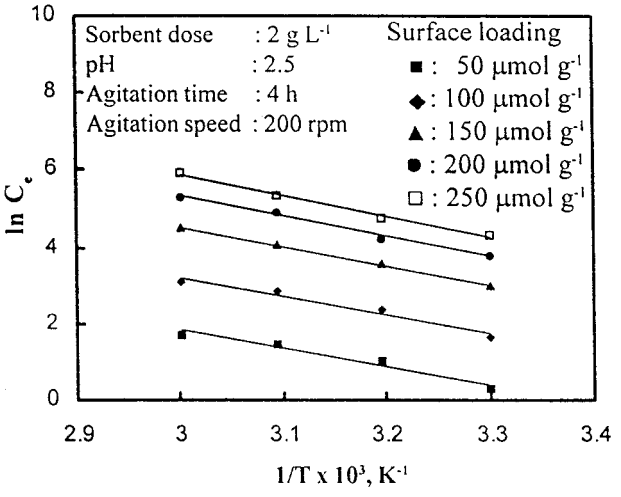

Figure 10 Plots of ln C_e for phosphate at constant amount adsorbed as a function of $1/T$.

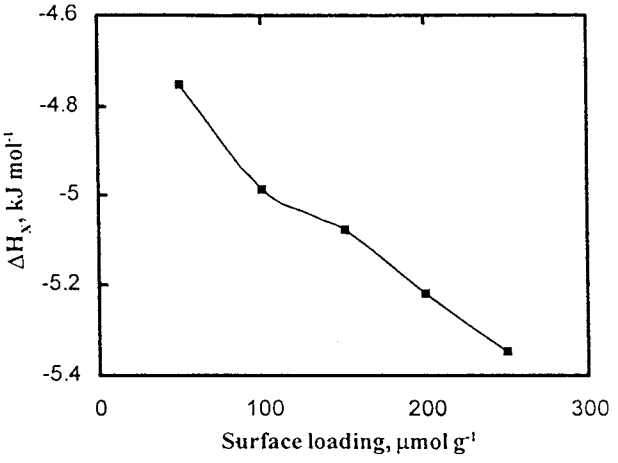

Figure 11 Variation of ΔH_x with respect to surface loading.

Table III Extraction of Phosphate from Phosphate Adsorbed S—$Fe(OH_2)_2$

Extractant (0.1*M*)	Desorption (%)
$NaNO_3$	33.8
NaCl	34.5
Na_2SO_4	73.6
HCl	36.8
HNO_3	28.7
H_2SO_4	30.4
NaCl—HCl	41.4
NH_4NO_3—HNO_3	50.8
NaOH	96.8

the presence of some lateral interactions between adsorbed molecules.

Desorption Studies

Solutions of $NaNO_3$, NaCl, Na_2SO_4, HCl, HNO_3, NaCl—HCl, H_2SO_4, NH_4NO_3—HNO_3, and NaOH were evaluated for the extraction of phosphate from S—$Fe(OH_2)_2$ into the aqueous phase again. The desorption results are presented in Table III. Among the various extractants used, NaOH has been found to be a good reagent for the desorption of phosphate. This may be attributed to the displacement of phosphate ions bound to the adsorbent with OH^- ions during the extraction stage. An efficiency of 96.8% was obtained by using 0.1*M* NaOH and is suitable for the quantitative extraction of phosphate into the aqueous phase.

Test with Industrial Wastewater

The utility of the adsorbent material was demonstrated by treating it with real industrial wastewater. Industrial wastewater collected from the local fertilizer industry was characterized using standard methods[15] and the composition is given in Table IV. The amount of phosphate in the industrial wastewater was found to be very low

Table IV Composition of Industrial Wastewater

Composition (μmol L^{-1}):
Pb^{2+}: 14.96; Hg^{2+}: 3.49; Cd^{2+}: 10.66; Cl^-: 3943.66;
NO^{3-}: 1064.52; NO^{2-}: 239.13; SO_4^{2-}: 1666.66;
PO_4^{3-}: 68.85; total NH_3: 16235.2; F^-: 578.94; total
hardness: 720; COD: 3687.5; BOD: 2656.25;
dissolved oxygen: 115.63; As(III): 50.66; pH: 4.3
(suspended solid: 228.5 mg/L)

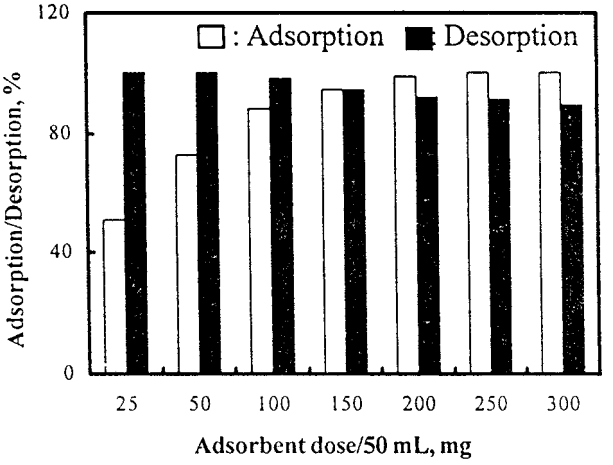

Figure 12 Effect of adsorbent dose for the removal of phosphate from industrial wastewater by S—$Fe(OH_2)_2$.

(68.85 μmol L^{-1}) and, hence, it was spiked with a phosphate solution, so that the final concentration of phosphate was 250 μmol L^{-1}. Figure 12 shows the influence of the adsorbent dose on the phosphate removal from wastewater by S—$Fe(OH_2)_2$. It is evident that for quantitative removal of phosphate ions from 50 mL industrial wastewater containing 250 μmol L^{-1} and several other ions an adsorbent dosage of 2 g L^{-1} is sufficient for the removal of 89.5% of the total phosphate, which is in good agreement with those obtained from the batch experiments mentioned above. It is apparent that by increasing the adsorbent dose from 0.5 to 5 g L^{-1} the removal efficiency increases. Similar adsorbent concentration effects were observed by earlier workers[33] in the adsorption of arsenate from wastewater by an industrial solid waste. The adsorbent dose for the 99.8% removal of phosphate from wastewater was found to be 4 g L^{-1}. Under these conditions, the lowest phosphate concentration attained by this material was 0.50×10^{-3} mmol L^{-1}. The permissible limit of phosphate for the discharge of wastewater[34] is 0.03 mmol L^{-1}. Hence, this adsorbent can be effectively used for the treatment of phosphate-containing wastewater. The data can also be used to derive a mathematical relationship, to relate the phosphate removal to the adsorbent dose (using adsorbent dose m_s = 0.5 to 5 g L^{-1}). This relationship, for which the correlation coefficient (r) was 0.99, is

$$R = \frac{m_s}{5.319 \times 10^{-3} + 8.818 \times 10^{-3} m_s} \quad (11)$$

Table V Desorption and Regeneration Data

No. Cycles	Adsorption (%)	Recovery (%)
1	88.0	98.2
2	83.6	95.6
3	79.1	92.8

This equation can be used to predict the percentage removal of phosphate for any adsorbent dose within the test limits at pH 2.5 and an initial phosphate concentration of 250 μmol L^{-1}.

Regeneration Studies

The adsorbed phosphate was removed using 0.1*M* NaOH. An above 98.0% recovery was achieved using 0.1*M* NaOH (Fig. 12). Table V summarizes the results of desorption and regeneration of S—$Fe(OH_2)_2$. After three cycles, the adsorption capacity of S—$Fe(OH_2)_2$ was reduced by 8.9% and recovery of phosphate ions in 0.1*M* NaOH decreased from 98.2% in the first cycle to 92.8% in the third cycle. About a 3% sorbent weight loss was observed after NaOH treatment. The results show that the spent adsorbent can be readily regenerated for repeated use with very little loss of weight of the adsorbent material.

CONCLUSIONS

Iron(III)-loaded carboxylated polyacrylamide-grafted sawdust was found to be a suitable adsorbent for the removal of phosphate from an aqueous solution. The sorption is pH-dependent and best results were obtained at pH 2.5. The maxima in removal of 97.6 and 90.3% was observed at pH 2.5 for initial concentrations of 100 and 250 μmol L^{-1}, respectively. The ligand-exchange reaction between the coordinated water and the phosphate ($H_2PO_4^-$) ions is the major removal mechanism involved. The adsorption follows second-order kinetics. Kinetic parameters were calculated in order to predict the nature of adsorption. Intraparticular diffusion was found to be the rate-limiting step. The adsorption capacity increased with increase of the temperature. The equilibrium in the adsorbent/phosphate ion solution systems was described by the Langmuir adsorption isotherm. The isosteric heat of adsorption decreased with increase of the surface loading. Carbonate at a concentration of 1000 μmol L^{-1} interfered with sorption to a maximum extent. Utility of the adsorbent was tested using fertilizer industry wastewater. The adsorption density, in general, decreased as the adsorbent dose increased from 0.5 to 5 g L^{-1}. The spent adsorbent can be regenerated and reused by alkali treatment. Ongoing investigations are aimed at developing an effective method for the disposal of the adsorbent after its utilization. The results of the investigations are quite useful for the removal of phosphate from wastewaters using batch or stirred tank flow reactors.

The authors are thankful to the Head, Department of Chemistry, University of Kerala, Trivandrum, for providing the laboratory facilities.

REFERENCES

1. Shukla, S. S.; Syers, J. K.; Williams, J. D. H.; Armstrong, D. E.; Harris, R. F. Soil Sci Soc Am Proc 1971, 35, 244.
2. Vanloon, G. W.; Duffy, S. J. Environmental Chemistry: A Global Perspective; Oxford University: New York, 2000.
3. Bhargava, D. S.; Sheldkar, S. B. Wat Res 1993, 27, 313.
4. Sreenivasalu, A.; Sundaram, E. V.; Kamal Reddy, M. Indian J Chem Technol 1999, 6, 256.
5. Brattebo, H.; Odegward, J. Wat Res 1986, 20, 977.
6. Roques, H.; Jeddy, N.; Libuglf, A. Wat Res 1991, 25, 1991.
7. Palanivelu, K.; Elangovan, N. Indian J Environ Protec 1994, 14, 688
8. Manju, G. N.; Anirudhan, T. S. J Sci Ind Res 2000, 59, 144.
9. Suzuki, T. M.; Itabashi, O.; Goto, T.; Yokoyama, T.; Kimura, T. Bull Chem Soc Jpn 1987, 60, 2839.
10. Raji, C.; Anirudhan, T. S. Indian J Chem Technol 1996, 3, 345.
11. Sreedhar, M. K.; Anirudhan, T. S. J Appl Polym Sci 2000, 75, 1261.
12. Beas, A. U.; Okuda, T.; Nishijima, W.; Shoto, C.; Okada, M. Wat Sci Technol 1997, 35, 89.
13. Yoshida, I.; Takashita, R.; Ueno, K. Bull Chem Soc Jpn 1984, 57, 54.
14. Maya, R. U.; Anirudhan, T. S. Ind Eng Chem Res 2001, 40, 2693.
15. APHA; Standard Methods for the Examination of Water and Wastewater, 18th ed.; APHA, AWWA, and WEF: Washington, DC, 1992.
16. Viladkar, S.; Agarwal, R.; Kamaludhin, B. Bull Chem Soc Jpn 1996, 69, 95.
17. Schwarz, J. A.; Driscoll, C. T.; Bhanot, A.K. J. Colloid Interf Sci 1984, 97, 55.
18. Borida, A. J Polym Sci A 1969, 2, 1761.
19. Kotau, M. M.; Sazamov, Y. N. Polym Sci USSR 1973, 15, 857.

20. Honeyman, B. D.; Santschi, A. H. Environ Sci Technol 1988, 22, 862.
21. Vujakovic, A. D.; Tomasevic-Canovic, M. R.; Dakovic, A. S.; Dondur, V. T. Appl Clay Sci 2000, 17, 265.
22. Kudesia, V. P. Pollution; Pragati Prakashan: Meerut, 1990.
23. Kuo, S.; Lotse, E. G. Soil Sci Soc Am Proc 1974, 38, 30.
24. Sreenivasa Rao, M.; Bandyopadhyay, M. Indian J Environ Mgmt 1995, 22, 124.
25. Laidler, K. J. Chemical Kinetics; McGraw-Hill: New York, 1965.
26. Knocke, W. R.; Hemphill, L. H. Wat Res 1981, 15, 275.
27. Griffin, R. A.; Jurinak, J. J. Soil Sci Soc Am Proc 1973, 37, 869.
28. Giles, C. H.; McEwan, T. H.; Nakhwa, S. N.; Smith, D. J Chem Soc 1960, 4, 3973.
29. Gupta, S. P. Statistical Methods; Sultan Chand: New Delhi, 1987.
30. James, B. R.; Rabenhorst, M. C.; Frigon, G. A. Wat Environ Res 1992, 64, 699.
31. Cheung, K. C.; Venkitachalam, T. H.; Scott, W. D. Wat Sci Technol 1994, 30, 247.
32. Young, D. M.; Growell, A. D. Physical Adsorption of Gases; Butterworth: London, 1962.
33. Namasivayam, C.; Senthikumar, S. Ind Eng Chem Res 1998, 37, 4816.
34. Galarneau, E.; Gehr, R. Wat Res 1997, 31, 328.